Thermooptical Sensitivity Analysis of Highly Birefringent Polarimetric Sensing Photonic Crystal Fibers With Elliptically Elongated Veins

Nikolaos J. Florous, *Member, IEEE*, Shailendra K. Varsheney, *Member, IEEE*, Kunimasa Saitoh, *Member, IEEE*, and Masanori Koshiba, *Fellow, IEEE*

***Abstract*—The spectral and thermooptical sensitivity responses of highly birefringent photonic crystal fibers (PCFs) with elliptically elongated veins integrated in their profile are being investigated using a novel sensitivity analysis based on an accurate semivectorial modal solver combined with temperature-dependent Sellmeier equations for pure silica and dry air. We demonstrate that by an appropriate selection of the design parameters it is possible to optimize the sensitivity of the modal birefringence or even to obtain null response at specific wavelengths. Thus, our investigation adds evidence to the potential use of highly birefringent PCFs as polarimetric sensors. Optimized overall temperature sensitivity could be obtained up to $7.5 \cdot 10^{-7}\mathrm{K}^{-1}$ at operational wavelength of 1.55 μ m.**

***Index Terms*—Photonic crystal fibers (PCFs), polarimetric sensors, sensitivity analysis, temperature-dependent Sellmeier equations, virtual boundary method.**

I. INTRODUCTION

INDEX GUIDING photonic crystal fibers (PCFs), also known as holey fibers, are novel optical waveguides based on an artificially periodic microstructured profile that can enable light to be controlled in the fiber in ways not previously possible or even imaginable. They have attracted considerable attention in recent years [1], due to the unlimited possibilities in engineering their modal properties. Despite their great significance in various applications proposed so far, there are not yet scientific reports on the use of PCFs as polarimetric sensors [2]–[5], mainly for two reasons. First, a sensitivity analysis which permits the calculation of thermooptical responses in PCFs is not known, and second, until now, temperature-independent Sellmeier equations were used so far to describe their material properties, thus prohibiting temperature-dependent phenomena to be studied in PCFs. In this letter, we report the first complete theoretical study of thermooptical responses in PCFs with elliptical elongated veins integrated in their profile and we identify novel mechanisms that contribute to the overall thermooptical response of PCF-based polarimetric sensors.

The response of classical Bragg grating sensors or polarimetric fiber sensors to external stress, temperature, and pressure primarily stems from a change in the refractive index of glasses induced by strain. In a more accurate consideration, one also needs to account for the dynamic rate of change in the refractive index caused by additional factors than strain as well as for the geometrical deformation of the cross profile of the fiber. For instance, the change of temperature induces strain due to the nonuniform expansion of the fiber's cross profile, which in turn affects the distribution of refractive index in the fiber. Although this is the primary mechanism responsible for the change of measured parameters such as the modal index and birefringence in a classical fiber sensor, if a standard highly birefringent fiber sensor is replaced by a PCF, temperature no longer introduces strain. Now other secondary effects become dominant and can alter the thermooptical response of PCF-based sensors, namely the temperature dependencies of the refractive indexes of silica and air as well as the cross profile's thermal expansion.

II. MODELING THE THERMOOPTICAL SENSITIVITY RESPONSE IN HIGHLY BIREFRINGENT PCFs

For PCFs, the thermal-induced strain is negligible, since the thermal expansion is considered uniform. The change of the fiber birefringence B with temperature T can be expressed using the contributions from the thermal refractive index change and from the thermal expansion as

$$\begin{aligned}\frac{dB}{dT} &= \frac{\partial B}{\partial l}\frac{\partial l}{\partial T} + \frac{\partial B}{\partial n_s}\frac{\partial n_s}{\partial T} + \frac{\partial B}{\partial n_h}\frac{\partial n_h}{\partial T} \\ &= \frac{\partial B}{\partial l} l a_s + \frac{\partial B}{\partial n_s}\beta_s + \frac{\partial B}{\partial n_h}\beta_h \end{aligned} \tag{1}$$

where in (1) we have accounted for the thermal expansion l as well as for the thermal change of the refractive indexes of silica n_s and the material inserted in the holes n_h. The significance of effects related to thermal expansion and to the change of refractive indexes are governed by the respective coefficients, namely by the thermal expansion coefficient of silica $a_s = 5.5 \times 10^{-7}\mathrm{K}^{-1}$ and the thermal coefficients of both silica $\beta_s = 1.2 \times 10^{-5}\mathrm{K}^{-1}$ and the dry-air $\beta_h = -0.9 \times 10^{-6}\mathrm{K}^{-1}$. The above parameters related to (1) have been estimated during differentiation from the knowledge of temperature-dependent Sellmeier equations for both pure silica [6], [7] as well as for dry-air [8]. These equations can be summarized as follows:

$$n_s^2 = A + \frac{B\lambda^2}{\lambda^2 - C} + \frac{D\lambda^2}{\lambda^2 - E} \tag{2}$$

Manuscript received April 11, 2006; revised May 10, 2006.

N. J. Florous is with the Division of Media and Network Technologies, Hokkaido University, Sapporo 060-0814, Japan (e-mail: nflorous@dpo7.ice.eng.hokudai.ac.jp).

S. K. Varsheney, K. Saitoh, and M. Koshiba are with the Division of Media and Network Technologies, Hokkaido University, Sapporo 060-0814, Japan.

Digital Object Identifier 10.1109/LPT.2006.879543

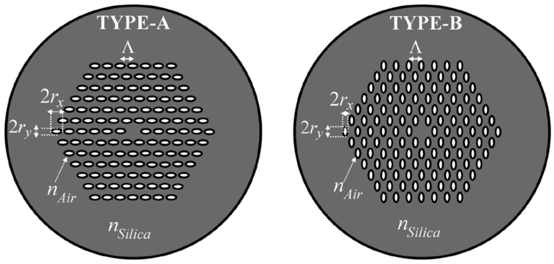

Fig. 1. Schematic cross section of the highly birefringent PCFs considered as polarimetric sensors, (left panel) type-A PCF with horizontally oriented elliptical air holes, and (right panel) type-B PCF with vertically oriented elliptical air holes.

where the constants A, B, C, D, and E are linearly dependent on temperature-T (in Celsius) in the following manner:

$$A = M_A T + Y_A; M_A = 3.1463 \times 10^{-8}; Y_A = 1.3155$$
$$B = M_B T + Y_B; M_B = 2.0427 \times 10^{-5}; Y_B = 0.7884$$
$$C = M_C T + Y_C; M_C = 2.8155 \times 10^{-6}; Y_C = 0.011029$$
$$D = M_D T + Y_D; M_D = -6.7886 \times 10^{-5}; Y_D = 0.91136$$
$$E = M_E T + Y_E; M_A = 100; Y_E = 10^{-10}.$$

For dry-air with standard volumetric composition of: 78.03% nitrogen (N), 20.99% oxygen (O_2), 0.03% carbon dioxide (CO_2), 0.01% hydrogen (H_2), and 0.94% argon (Ar), the corresponding temperature-dependent Sellmeier equation takes the following form [8]:

$$n_h(T) = 1 + 10^{-8}\left(6432.8 + \frac{2949810\lambda^2}{146\lambda^2 - 1} + \frac{25540\lambda^2}{41\lambda^2 - 1}\right) \times \left(\frac{1 + aT_s}{1 + aT}\right)\frac{P}{P_s} \quad (3)$$

where in the above equation T is the temperature in Celsius, $T_s = 15$ °C is a reference temperature, λ is the wavelength in μm, P is the pressure in mm-Hg, P_s = 760-mm Hg is the reference standard pressure under normal conditions, and a is a parameter slowly varying with temperature and can be depicted from [8] for different wavelength bands.

For PCF sensors, there are at least two novel sensing mechanisms that are not present in standard fiber sensors. First since the change of the refractive index of air holes with temperature is by an order of magnitude smaller than that of silica and has an opposite sign, the thermal response of PCF-sensors partly results from the direct nonuniform change of the refractive indexes from its cross profile. Second the large refractive index contrast between air and silica emphasizes the geometrical changes within the cross profile, as compared to the case of standard fibers. In our investigation, we combine a rigorous semivectorial technique of virtual boundary method [9] for the accurate prediction of the modal characteristics of PCFs with elliptically elongated air holes, with (1)–(3), to form an accurate algorithm for the thermooptical sensitivity prediction in PCFs. As shown in Fig. 1, we consider PCFs with elliptical air holes arranged in a triangular configuration with lattice constant Λ, and filling ratio f (the ratio of the major semi axis over the pitch constant), while we particularly distinguish them in two types: type-A where the orientation of the major axis of the elliptical air holes is across the x-axis (horizontal axis), and type-B with corresponding orientation across the y-axis (vertical axis). In both cases the ellipticity is considered uniform across the profile of the PCFs and defined always as the ratio of the major semi axis over the minor semiaxis. The choice of PCFs with elliptical air holes is considered here for mainly three reasons. At first it is well known that the use of elliptical deformations can significantly enhance the modal birefringence to very high values [9], [10]. The second reason is that their refractive index profile is much simpler to realize [11] in comparison to other highly birefringent PCFs with dissimilar air holes [12]. The third and most important reason is that the optimization of the sensitivity of the modal birefringence can be controlled using only one parameter, that is the ellipticity of the air holes as will be demonstrated later.

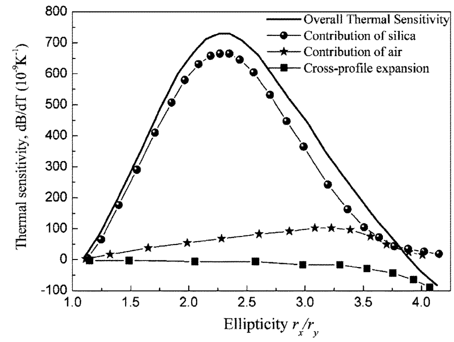

(a)

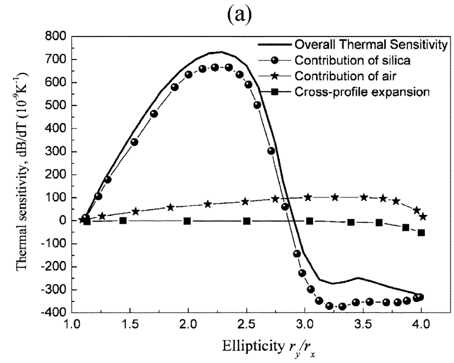

(b)

Fig. 2. Contributions of silica (circles), air (stars), and the cross profile expansion of the geometry (squares), to the overall thermal sensitivity (solid curve) of the modal birefringence (K^{-1}), at $\lambda = 1550$ nm, as a function of the air-hole ellipticity-e for (a) type-A PCF and (b) type-B PCF. For both cases, the maximization of the sensitivity function occurs for an air-hole ellipticity value of $e = 2.27$.

III. Selected Numerical Results and Discussion

Fig. 2 shows the contributions of silica (circles), air (stars), and the cross profile expansion of the geometry (squares), to the overall thermal sensitivity (K^{-1}) (solid curve) of the modal birefringence, as a function of the air-hole ellipticity for (a) type-A PCF and (b) type-B PCF. For both cases the following design parameters are considered: $\Lambda = \lambda/2$, filling ratio $f = 22.8\%$, the ellipticity of the air holes is set as variable, while the operational wavelength $\lambda = 1550$ nm. Note that in the case of Fig. 2(a) there is a positive value of the overall sensitivity for a wide range of ellipticities, as opposed to the usual case of polarimetric fiber sensors. This result clearly indicates a significant difference in the physical mechanism behind sensing using PCFs. For the y-oriented air holes, there exists a threshold value of the ellipticity, after which, the sensitivity drops to negative values and thus it can provide the possibility for designing a sensor having ideal temperature compensation. Perhaps one

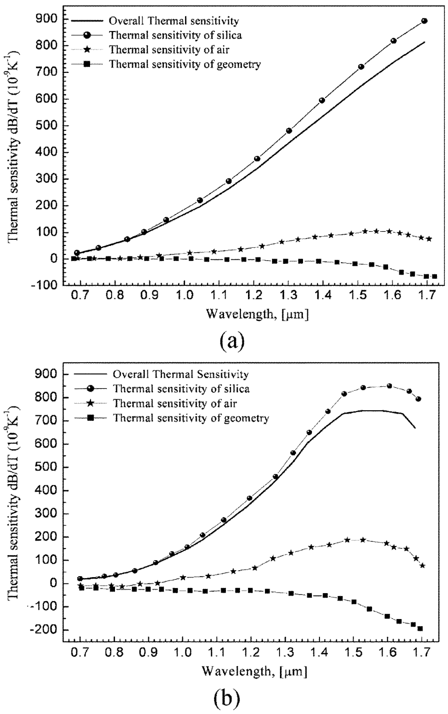

Fig. 3. Thermal sensitivity of the modal birefringence (K^{-1}) of silica (circles), air (stars), and the cross profile expansion of the geometry (squares), as a function of the operational wavelength λ in (μm), for (a) type-A PCF and (b) type-B PCF at fixed ellipticity of $e = 2.27$.

of the remarkable results is that for both cases the sensitivity of the modal birefringence takes its maximum value at ellipticity of $e = 2.27$. Near the region of zero-crossing, the main mechanism contributing to the overall sensitivity is not only the change of the refractive index of silica but also that of air. At the exact point of zero-crossing, it is evident that all these contributions are in balance. Fig. 3 shows the calculated contributions of silica (circles), air (stars), the cross profile expansion of the geometry (squares), to the overall thermal sensitivity (K^{-1}) (solid curve) of the modal birefringence, as a function of the operational wavelength λ and for fixed air-hole ellipticity of $e = 2.27$, for (a) type-A PCF and (b) type-B PCF. We can see that in the case of Fig. 3(b), the sensitivity of the modal birefringence reaches a global maximum with a value of about 7.5×10^{-7} K^{-1} around the telecommunication band, while in case of (a) is monotonically increasing. In Fig. 4, we plot the modal field intensity of the fundamental mode for PCFs with $\Lambda = \lambda/2$, filling ratio $f = 22.8\%$, calculated at maximum thermal sensitivity and for operational wavelength of $\lambda = 1550$ nm, for type-A PCF (left panel) and type-B PCF (right panel), while we consider a total number of six air-hole rings. Although from the results in Fig. 4 it seems that the confinement loss is quite high, we may drastically reduce it by increasing the number of air-hole rings (around 12).

IV. Conclusion

To summarize our work, the virtual boundary method was used in combination with temperature-dependent Sellmeier

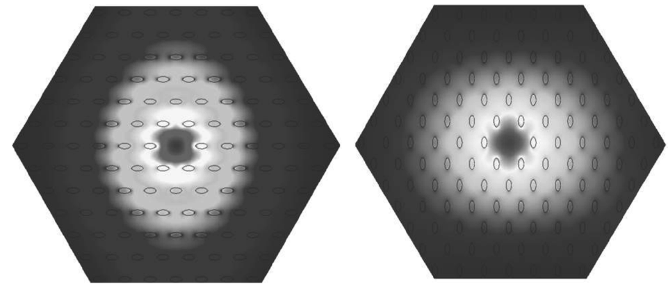

Fig. 4. Normalized intensity distributions of the fundamental mode calculated at maximum thermal sensitivity and for operational wavelength of $\lambda = 1550$ nm, for type-A PCF (left panel) and type-B PCF (right panel). The total number of air-hole rings is six for both cases.

equations to form a rigorous computational technique for the accurate estimation of thermal sensitivities in PCFs. We saw that PCFs can be potentially used as polarimetric sensors. The results obtained here are consistent with reported experimental results on PCFs [13]. Further investigations regarding different types of PCFs with infiltered noble gasses in the air holes, are currently under consideration.

References

[1] J. Broeng, D. Mogilevtsev, S. E. Barkou, and A. Bjarklev, "Photonic crystal fibers: A new class of optical waveguides," *Opt. Fiber Technol.*, vol. 5, pp. 305–330, Jul. 1999.
[2] K. Mochizuki, Y. Namihira, and Y. Ejiri, "Birefringence variation with temperature in elliptically cladded single-mode fibers," *Appl. Opt.*, vol. 21, pp. 4223–4228, Dec. 1982.
[3] A. Wang, G. Wang, K. Murphy, and R. Claus, "Refractive index and material dispersions of multi-component oxide glasses," *Opt. Lett.*, vol. 17, pp. 1391–1393, Oct. 1991.
[4] C. E. Lee, R. Atkins, and H. F. Taylor, "Performance of fiber optic temperature sensor from -200 to 1050 °C," *Opt. Lett.*, vol. 13, pp. 1038–1040, Nov. 1988.
[5] W. Bock and T. Eftimov, "Polarimetric and intermodal interference sensitivity to hydrostatic pressure, temperature, and strain to highly birefringent optical fibers," *Opt. Lett.*, vol. 18, pp. 1979–1981, Nov. 1993.
[6] G. Ghosh, *Handbook of Thermo-Optic Coefficients of Optical Materials with Applications*. San Diego, CA: Academic, 1997.
[7] T. Mito, S. Fujino, H. Takebe, K. Morinaga, S. Todoroki, and S. Sakaguchi, "Refractive index and material dispersions of multi-component oxide glasses," *J. Non-Cryst. Solids*, vol. 210, pp. 155–162, Aug. 1997.
[8] R. Penndorf, "Table of the refractive index of standard air and the Rayleigh coefficient for the spectral region between 0.2 and 20 μm and their application to atmospheric optics," *J. Opt. Soc. Amer.*, vol. 47, pp. 176–182, Feb. 1957.
[9] N. Florous and M. Koshiba, "Virtual boundary method for the analysis of elliptically cross-sectional photonic crystal fibers with elliptical pores," *J. Lightw. Technol.*, vol. 23, no. 4, pp. 1763–1773, Apr. 2005.
[10] M. J. Steel and R. M. Osgood, "Polarization and properties of elliptical-hole photonic crystal fibers," *J. Lightw. Technol.*, vol. 19, no. 4, pp. 495–502, Apr. 2001.
[11] N. A. Issa, M. A. Eijkelenborg, M. Fellew, F. Cox, G. Henry, and C. J. Large, "Fabrication and study of microstructured optical fibers with elliptical holes," *Opt. Lett.*, vol. 29, pp. 1336–1338, Jun. 2004.
[12] A. Ortigosa-Blanch, J. C. Knight, W. J. Wadsworth, J. Arriaga, B. J. Mangan, T. A. Birks, and P. St. J. Russell, "Highly birefringent photonic crystal fibers," *Opt. Lett.*, vol. 25, pp. 1325–1327, Sep. 2000.
[13] S. Konorov, A. Zheltikov, and M. Scalora, "Photonic crystal fiber as a multifunctional optical sensor," *Opt. Express*, vol. 13, pp. 3454–3459, May 2005.